ELSEVIER

Polymer 44 (2003) 295–306

polymer

www.elsevier.com/locate/polymer

Copolymerization of ethylene and styrene by homogeneous metallocene catalysts. 1. Theoretical studies with *rac*-ethylenebis-(tetrahydroindenyl)MCl_2 [M = Ti, Zr] systems

S. Martínez[a], V. Cruz[b], A. Muñoz-Escalona[a], J. Martinez-Salazar[a,*]

[a]*Instituto de Estructura de la Materia, GIDEM, CSIC, c/Serrano, 113bis, 28006 Madrid, Spain*
[b]*Centro Técnico de Informática, CSIC, c/Pinar, 19, 28006 Madrid, Spain*

Received 31 July 2002; received in revised form 16 October 2002; accepted 16 October 2002

Abstract

A computational study of the ethylene–styrene copolymerization with *rac*-ethylenebis(tetrahydroindenyl)MCl_2 [M = Ti, Zr] systems using DFT methods is presented. The complexation, coordination and insertion energies for ethylene and styrene monomers as well as for the styrene–ethylene copolymerization steps into the catalytic active site models $[Et_2(IndH_4)_2]MCH_3^+$ [M = Ti, Zr] were calculated. The goal of this study is to examine the influence of the metal atom [Ti, Zr] on the copolymerization activity. It could be concluded that zirconocene catalyst is much more active than the titanocene based catalyst. This could be explained by the higher steric congestion around the Ti as compared to the Zr complex. Furthermore, it was found that the primary styrene insertion gives rise to complexes in which the active sites are blocked by the phenyl ring in both metal atoms, so that only the secondary insertion of the styrene is possible. These facts might help to clarify the already published experimental results.

Keywords: Ethylene–styrene copolymerization; Metallocene catalysts; Density functional study

1. Introduction

Over last decades many attempts have been made to synthesise Ethylene (E)–Styrene (S) copolymers. Due to the multiple active site nature, traditional Ziegler–Natta catalysts are unable to copolymerise ethylene with styrene, producing in general a mixture of ethylene homopolymer, polyethylene with low content of styrene comonomer (less than 1.0 mol%) and styrene block copolymer [1–3]. Only just with the discovery of homogeneous single-site metallocene catalysts, E–S copolymers have been synthesised covering a broad range of compositions and structures [4–6]. Among the metallocene catalysts, titanium based complexes are the most widely and efficient known systems to promote E–S copolymerization [7–9]. Regarding the Zr based metallocene catalysts the so-called Ewen type metallocene catalysts is one of the first example reported for the copolymerization of E and S [10,11]. More recently, the well known catalytic system *rac*-ethylenebis(1-indenyl)zirconium dichloride activated by methylalumionxane [12,13], as well as others bridged Zr based catalysts have been reported for the synthesis of E–S copolymers [14].

Our interest is to explore the effect that the metal atom and the structure of the catalytic organometallic complex could have on the copolymerization activity and on the structure and properties of the resulting E–S copolymers. In this effort, we are extensively using computer modelling. It should be pointed out that despite the great amount of publications on the theoretical modelling of polymerization using metallocene catalysts, little attention has been paid to ethylene–styrene copolymerization.

In a previous paper [15] we have published the theoretical modelling of the well-known $CpTiCl_3$ catalyst used for E–S copolymerization. Special attention was devoted to the role of the oxidation state of the titanium metal, particularly when considering that under normal polymerization conditions Ti (IV) can be easily reduced to Ti (III), In this paper, we present the results obtained by the *rac*-ethylenebis(tetrahydroindenyl)MCl_2 [M = Ti, Zr] systems in order to study the influence of the two transition

* Corresponding author. Tel.: +34-915901618; fax: +34-915855413.
E-mail address: jmsalazar@iem.cfmac.csic.es (J. Martinez-Salazar).

0032-3861/03/$ - see front matter © 2002 Elsevier Science Ltd. All rights reserved.
PII: S0032-3861(02)00740-1

metal atoms on the catalytic activity. The results are discussed on the light of the published and current experimental results that will be presented elsewhere [16].

2. Computational methods

Energy calculations were performed within the density functional theory (DFT) formalism involving local density approximation [17] but adding non-local corrections to exchange [18] and correlation [19].

The LACV3P* basis set was used for all the calculations. It is an effective core potential basis set developed at Los Alamos National Laboratory [20]. LACV3P include the outermost set of core orbitals, i.e. 3s and 3p for titanium, along with a triple zeta contraction for the valence orbitals for every element developed and tested at Schrödinger, Inc., and polarization functions for non-hydrogen atoms.

Geometry optimisations were carried out with the following convergence criteria: 4.5×10^{-4} hartree/bohr as the maximum element of gradient, 3.0×10^{-4} hartree/bohr as the rms of gradient elements, 1.8×10^{-3} bohr as the maximum element of nuclear displacement. 1.2×10^{-3} bohr as the rms of nuclear displacement and 5.0×10^{-5} hartree as the energy difference between consecutive iterations.

Complexation energies were calculated as the difference between the optimised π-complex on one hand and cationic species and monomer on the other hand. Activation or insertion barriers were estimated as the energy difference between transition state structures and π-complex reactants.

The whole set of calculations were done with the Titan 1.0.5 software in a Pentium 4 based PCs.

3. Results and discussion

The optimized structures for the active species are shown in Fig. 1. There are two important differences between these geometries related to the size of the metal atom. Firstly, the distance metal-Cp centroid is on average, about 0.16 Å shorter in the titanocene than in the zirconocene case (2.061 vs. 2.223 Å for the longest distance, see Fig. 1) and secondly the angle Cp_centroid-Metal-Cp_centroid is 13° wider for the titanocene as compared to the zirconocene catalyst (140.7 vs. 127.6°, see Fig. 1). These two facts seems to indicate that the zirconium based species has more room at the active site than the titanocene species. These observations have important consequences for the copolymerization activities of both systems as it will be discussed below.

According to the monomer insertion (ethylene, 1,2 and 2,1 styrene) and copolymerization, this section has been divided in the following four parts: (1) ethylene insertion, (2) primary styrene insertion, (3) secondary styrene insertion and (4) ethylene–styrene copolymerisation.

3.1. Ethylene insertion

The complexation energy can be defined as the difference between the π-complex energy and the energies of the separated monomer and cationic species. The energy obtained for the ethylene complexation with the *rac*-$Et_2(IndH_4)_2Zr(CH_3)^+$ catalyst is −14.3 kcal/mol. The complexation energy for ethylene in the titanocene catalyst is −3.8 kcal/mol, which is significantly lower than for the zirconocene system (−14.3 kcal/mol). This fact can be explained by a 10° closing of the Cp_centroid–Ti–Cp_centroid angle respect to the cationic species in order to accommodate the incoming monomer (see Fig. 1 and Tables 1 and 2).

The complete path from separated reactants to most stable products for the initial ethylene insertion is presented in Figs. 2 and 3 for the Zr and Ti catalyst systems, respectively. Some geometrical parameters have been extracted and are given in Tables 1 and 2. The transition state for the insertion reaction presents the typical four centre pseudoring with the characteristic α-agostic interaction between a hydrogen attached to atom Cα and the Zr metal atom [21]. The energy barrier calculated for the ethylene insertion was 2.1 kcal/mol. The characteristic γ-agostic interaction formed after the insertion process is 12.9 kcal/mol more stable than the π-complex. This product can yield a more stable conformer by rotation of the growing polymer chain around the Cα–Cβ bond, giving rise to a structure presenting a β-agostic interaction which is

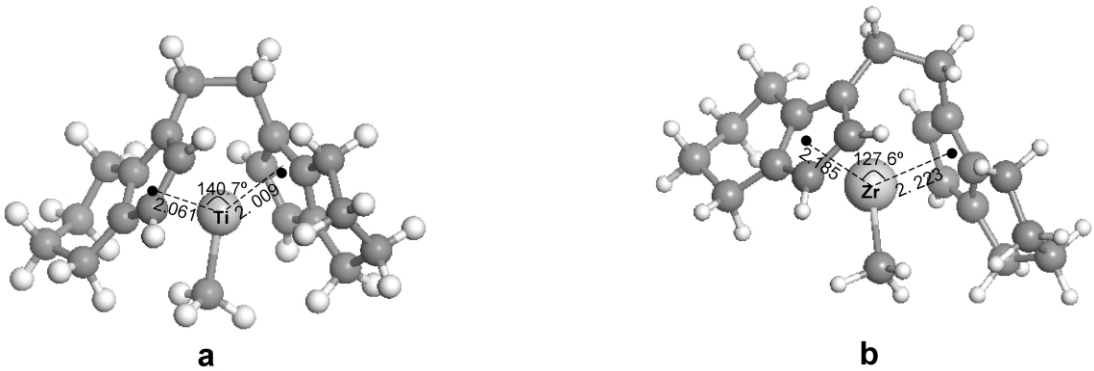

Fig. 1. Structures for the active cationic species: (a) *rac*-$Et_2(IndH_4)_2Ti(CH_3)^+$, (b) *rac*-$Et_2(IndH_4)_2Zr(CH_3)^+$.

Table 1
Geometric parameters for ethylene insertion into $[Et(IndH_4)]_2ZrCH_3^+$

	CpZrCp	Zr–Cp	Zr–Cp	Zr–C1et	Zr–CH_3	C1et–C2et	C2et–CH_3	Zr–Hγ	Zr–Hβ	Zr–Hα
π-Complex	126.5	2.234	2.244	2.856	2.260	1.356	3.185	–	–	–
Transition state	126.7	2.250	2.249	2.414	2.306	1.424	2.255	–	–	–
γ-Agostic product	126.7	2.228	2.218	2.233	2.695	1.567	1.569	2.265	–	–
β-Agostic product	129.3	2.208	2.187	2.259	3.976	1.532	1.542	–	2.244	–
α-Agostic product	127.8	2.209	2.193	2.215	4.696	1.531	1.543	–	–	2.316

3.1 kcal/mol lower in energy than the γ-agostic product. The rotational barrier for this process was not explicitly calculated but it has been estimated by other authors for similar metallocene systems to be around 1–2 kcal/mol [22]. Although the β-agostic compound is recognized as the resting state between successive monomer insertions, the appropriate precursor for further olefin polymerization is the α-agostic structure [23]. This conformer can be obtained by rotation of the growing polymer chain around the Zr–Cα bond which leads to a product 7.8 kcal/mol more unstable than the β-agostic one. A potential energy scan of the Zr–Cα rotation reveals a maximum 8.1 kcal/mol above the β-agostic structure. The corresponding transition state could not be calculated as the difference between the structure of the maximum in the potential energy scan and the α-agostic product is negligible. In every attempt to locate a transition state the algorithm always tends to give the α-agostic geometry. The rotational barrier was then estimated to be very similar to the energy difference between the β-agostic and α-agostic energies, being 7.8 kcal/mol. This product can be further stabilized by approaching a new ethylene molecule. The complexation energy due to a second monomer capture was calculated to be −14.7 kcal/mol. The reported energies and geometries are in agreement with those published in the literature for zirconocene systems at an equivalent level of theory [24].

A similar set of structures was obtained for the titanocene catalyst as can be seen in Fig. 3. Some small differences between both metallocenes can be inferred by comparing the data given in Figs. 2 and 3. The transition state obtained for the insertion process in the titanocene has the same characteristics described for the zirconocene based compound, namely a four centre pseudoring and the α-agostic interaction. The calculated insertion barrier into the Ti-alkyl bond is slightly lower than the corresponding to ethylene insertion into the zirconium analog (1.3 vs. 2.1 kcal/mol, respectively). Comparing atom–atom distances it is clear that the transition state in the titanocene occurs earlier in the reaction path than the corresponding saddle point structure located for ethylene insertion into the Zr based catalyst. The γ-agostic product formed after ethylene insertion in the Ti complex is 16.8 kcal/mol lower in energy than the π-complex, which is around 4 kcal/mol more exothermic than the corresponding reaction in the zirconocene case (−16.8 vs. −12.9 kcal/mol, see Figs. 2 and 3). Furthermore the corresponding β-agostic structure in the Ti compound is 5.9 kcal/mol more stable than the γ-agostic one and presents a −22.7 kcal/mol energy difference with respect to the π-complex. The β-agostic conformer in the titanocene is 6.7 kcal/mol more stable than the corresponding zirconocene conformer (−22.7 vs. −16.0 kcal/mol, respectively). The rotational barrier associated to the γ to β-agostic transformation was also estimated to be very small as in the zirconocene case. The α-agostic product can be obtained by rotation around the Ti-Cα bond. The calculated energy is 13.4 kcal/mol higher than the β-agostic interaction value. The corresponding barrier for the rotation around the Ti–Cα bond to get the α-agostic structure was estimated to be slightly above the difference between the β- to α-agostic energies. The location of the corresponding transition state was not possible due to the same reasons commented for the zirconocene system. The rotation of the growing polymer chain around the Ti–Cα bond seems to be the determinant step in the ethylene polymerization reaction based on the different energy values obtained for the whole process (complexation, insertion and alkyl chain rotation). Similar mechanism has also been proposed by other authors [25].

In case of the zirconocene catalyst the alkyl rotation barrier is around 8 kcal/mol while for the titanocene complex is 14 kcal/mol. Therefore, these activation energies are in agreement with the experimental values indicating

Table 2
Geometric parameters for ethylene insertion into $[Et(IndH_4)]_2TiCH_3^+$

	CpTiCp	Ti–Cp	Ti–Cp	Ti–C1et	Ti–CH_3	C1et–C2et	C2et–CH_3	Ti–Hγ	Ti–Hβ	Ti–Hα
π-Complex	130.5	2.084	2.086	2.627	2.152	1.359	2.842	–	–	–
Transition state	129.8	2.087	2.100	2.392	2.141	1.389	2.320	–	–	–
γ-Agostic product	130.5	2.052	2.078	2.106	2.644	1.555	1.560	2.137	–	–
β-Agostic product	132.2	2.021	2.049	2.131	3.890	1.517	1.545	–	2.120	
α-Agostic product	131.6	2.039	2.048	2.088	4.604	1.537	1.539	–	–	2.113

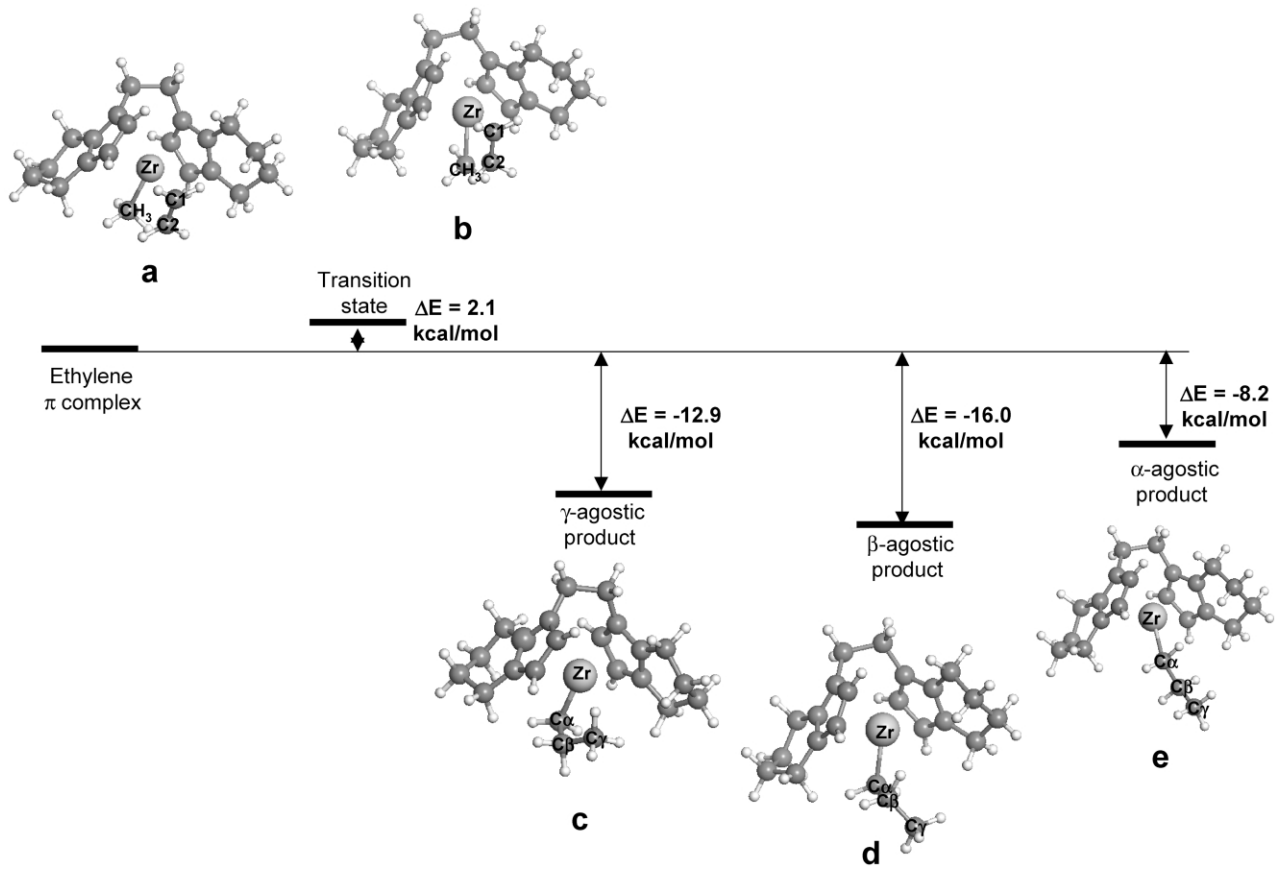

Fig. 2. Energy profile and structures for ethylene insertion into the *rac*-$Et_2(IndH_4)_2Zr(CH_3)^+$ catalyst.

that the zirconium based system is much more active for ethylene polymerization than the titanocene one [26].

A new ethylene molecule could be coordinated either to the α-agostic or to the β-agostic resting state. In the former case a propagation reaction should be expected to occur while in the second case a termination process would take place either by β-elimination or by β-hydrogen transfer to the monomer. For the titanocene species it was impossible to find an ethylene π-complex with the β-agostic conformer, so that chain termination is unlike to happen by this mechanism. Furthermore, the large stabilization obtained for the formation of the β-agostic structure in the $[Et_2(IndH_4)_2]TiCH_2CH_2CH_3^+$ molecule (−22.7 kcal/mol, see Fig. 3) suggests that β-elimination is also a difficult mechanism for chain termination. These findings are in agreement with the experimental fact indicating that polyethylene with higher molecular weight can be obtained with the titanocene catalyst as compared to the zirconocene one [27].

3.2. Primary styrene insertion

The styrene monomer can approach the cationic species in two different ways depending on the relative orientation of the tetrahydroindenyl ligands and the phenyl group of the monomer. Scheme 1 shows the different possibilities for both primary and secondary styrene coordination to the metal centre. For the primary styrene insertion into the zirconocene cation, the *re* coordination is 2.4 kcal/mol more stable than the *si* coordination, whereas for the titanocene the *si* coordination is 3.1 kcal/mol lower in energy than *re* coordination (see Scheme 1a). The difference in the preferred insertion mode found for the Zr compared to the Ti based system could be due to the steric interaction between the phenyl ring in the styrene monomer and the tetrahydroindenyl ligand. This interaction should be larger in the titanocene than in the zirconocene catalyst due to the size of the metal atom and the relative position of the tetrahydroindenyl groups. Furthermore, the *si* coordination should be, in principle, less hindered than *re* coordination for the 1,2 styrene complexation. Therefore, the Ti system seems to prefer the *si* coordination, whereas for the Zr catalyst the difference is smaller and even reversed in sign so that the *re* coordination is more stable than the *si* coordination.

For the zirconocene catalyst the *re* forms are the more stable for all 1,2 styrene polymerization steps (reactant, transition state and products). Although the *si* 1,2 styrene coordination was found to be slightly more stable than *re* coordination in the titanocene complex, the structures obtained for the transition state and products corresponding to the insertion process give energies for the *si* coordination

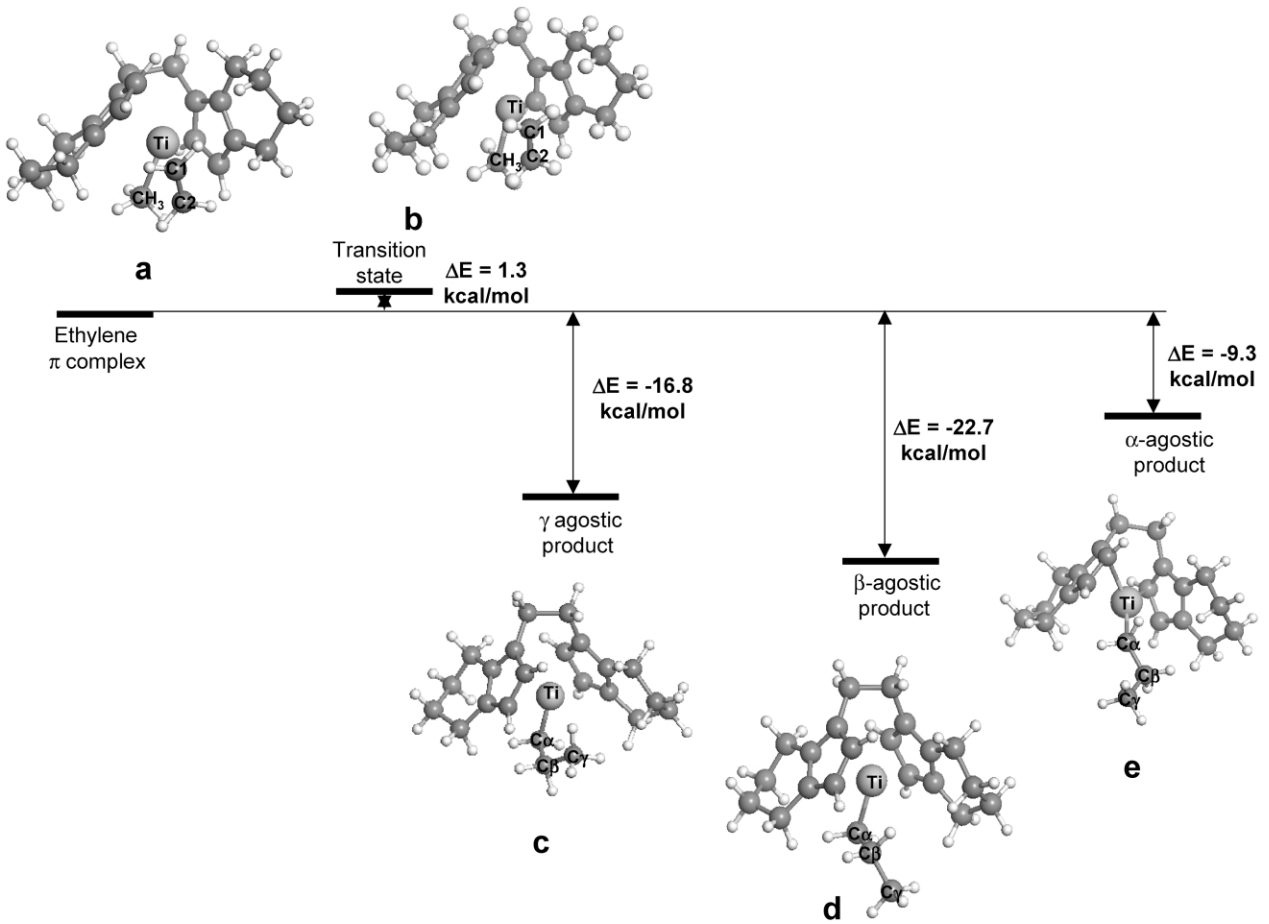

Fig. 3. Energy profile and structures for ethylene insertion into the *rac*-$Et_2(IndH_4)_2Ti(CH_3)^+$ catalyst.

consistently higher (about 4 kcal/mol) than the corresponding to *re* coordination geometries. Therefore, the simulations of 1,2 styrene insertion were performed based on the *re* π-complexes on both catalyst systems.

The complexation energy calculated for the 1,2 styrene π-complex for the zirconocene catalyst was −17.7 kcal/mol, which is somewhat larger than the value obtained for the ethylene complexation (−14.3 kcal/mol). In case of 1,2 styrene coordination to the titanocene catalyst the complexation energy is −7.2 kcal/mol, which is also higher than the value obtained for the ethylene monomer complexation (−3.8 kcal/mol).

The optimised geometries corresponding to the *re* 1,2 styrene insertion process into the $[Et_2(IndH_4)_2]ZrCH_3^+$ species are shown in Fig. 4. The transition state is 10.7 kcal/mol higher in energy than the π-complex reactant. The structure of the saddle point corresponds to the typical four member pseudo-ring found in metallocene systems. The calculated energy barrier is appreciably larger than the value obtained for ethylene insertion (2.1 kcal/mol), which is in agreement with the experimental findings indicating that styrene is more difficult to polymerise when compared to ethylene monomer [4,5] (Table 3).

The γ-agostic product obtained after 1,2 styrene insertion has an energy 1.5 kcal/mol above the π-complex reactant (Fig. 4c). This is an unusual result as this process generally exothermic. The rotation around the Cα–Cβ bond is an easy process giving a more stable product in which the phenyl

Table 3
Geometric parameters for 1,2 styrene insertion into $[Et(IndH_4)]_2ZrCH_3^+$

	CpZrCp	Zr–Cp	Zr–Cp	Zr–C1est	Zr–CH_3	C1est–C2est	C2est–CH_3	Zr–Hγ
π-Complex	126.2	2.242	2.243	2.611	2.273	1.377	3.251	–
Transition state	126.8	2.232	2.242	2.315	2.353	1.460	2.077	–
γ-Agostic product	127.1	2.228	2.219	2.246	2.705	1.555	1.578	2.238
Blocking product	125.3	2.272	2.238	2.313	4.070	1.571	1.547	–

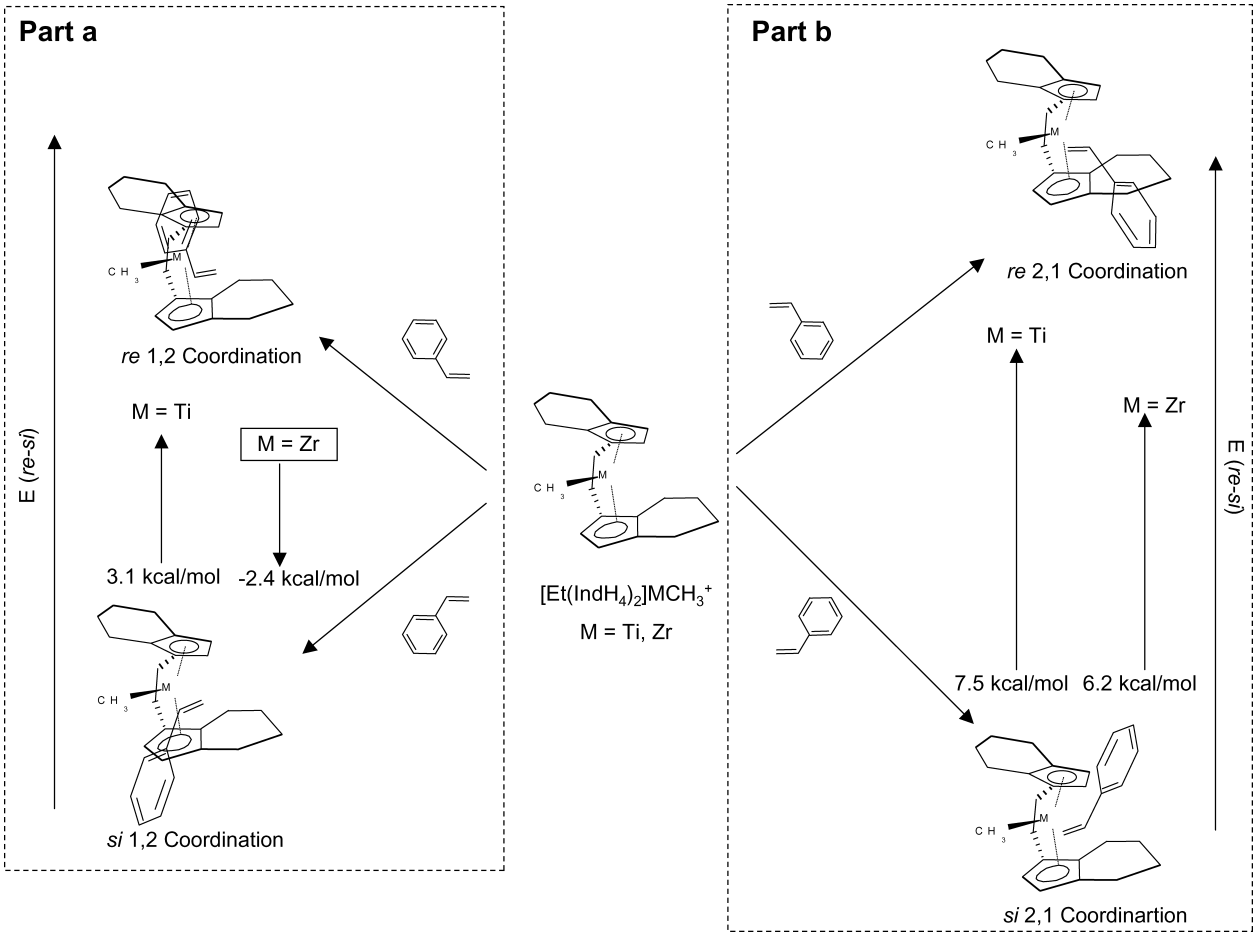

Scheme 1.

ring of the growing polymer chain is blocking the active site (Fig. 4d) and therefore avoiding any further monomer insertion. This structure is 4.3 kcal/mol more stable than the γ-agostic conformer. Furthermore, the β-agostic conformer cannot be formed due to the steric hindrance between the phenyl group in Cβ and the tetrahydroindenyl ligand.

The structures obtained for *re* 1,2 styrene insertion into the $[Et_2(IndH_4)_2]TiCH_3^+$ species can be shown in Fig. 5 and selected geometrical parameters are given in Table 4. The transition state for the insertion has an energy 6.3 kcal/mol above the reactant (Fig. 5b). This barrier is much lower than the corresponding to the same insertion into the zirconocene system (10.7 kcal/mol) but is still 5 kcal/mol higher than the activation energy calculated for ethylene insertion into the same catalyst. The γ-agostic product obtained is −7.3 kcal/mol more stable than the reactant in this case, which is the usual result found in the literature for olefin polymerization with metallocene systems. This structure can reorganize itself to a more stable form by rotation around the Cα–Cβ bond giving rise to a geometry where the active site is blocked by the phenyl group attached to Cβ of the growing polymer chain (Fig. 5d). The rotational barrier was estimated to be very small and the resulting structure is 4.7 kcal/mol more stable than the γ-agostic conformer in parallel with the results found for the zirconocene system.

Taking into account the above results for both catalyst systems, the 1,2 styrene insertion gives rise to inactive species avoiding any monomer polymerization.

Table 4
Geometric parameters for 1,2 styrene insertion into $[Et(IndH_4)]_2TiCH_3^+$

	CpTiCp	Ti–Cp	Ti–Cp	Ti–C1est	Ti–CH_3	C1est–C2est	C2est–CH_3	Ti–Hγ
π-Complex	129.5	2.105	2.111	2.429	2.138	1.379	3.201	–
Transition state	129.8	2.112	2.094	2.228	2.192	1.441	2.131	–
γ-Agostic product	131.0	2.072	2.044	2.122	2.799	1.561	1.553	2.190
Blocking product	130.2	2.098	2.094	2.175	4.424	1.565	1.539	–

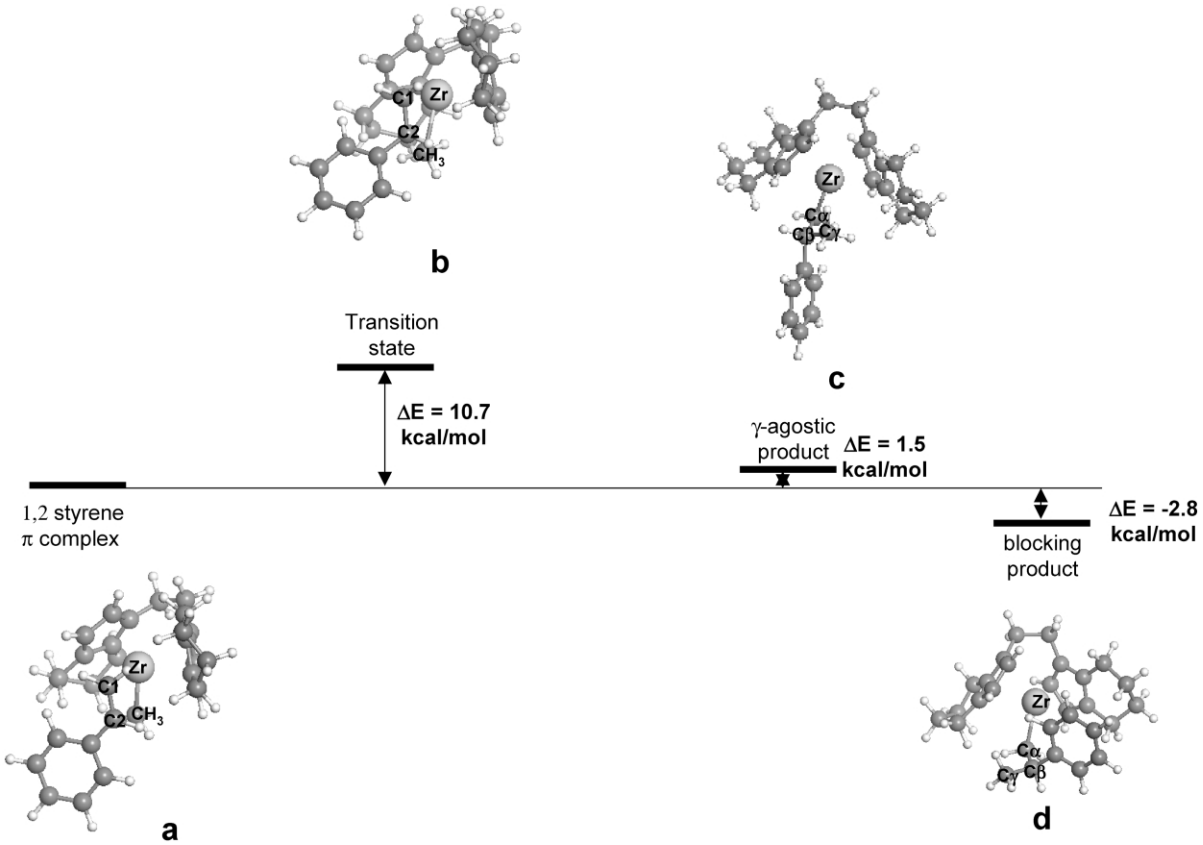

Fig. 4. Energy profile and structures for 1,2-styrene insertion into the *rac*-$Et_2(IndH_4)_2Zr(CH_3)^+$ catalyst.

3.3. Secondary styrene insertion

Scheme 1b shows the two possibilities of 2,1 styrene coordination to both metallocene systems. The *si* form is clearly more stable than the *re* coordination due to the fact that the phenyl group of the incoming monomer is less hindered by the tetrahydroindenyl ligands. The effect of the steric congestion around the metal centre is more noticeable here compared to the 1,2 styrene insertion, because the phenyl group of the monomer approaches very closely to the metal atom. Similar to the 1,2 styrene coordination, the energy difference between the *si* and *re* forms is larger in the titanocene case (7.5 kcal/mol) than in the zirconocene (6.2 kcal/mol) due to the smaller size of the Ti metal atom which makes the steric congestion larger with the Zr atom.

The complexation energy for 2,1 styrene insertion into the zirconocene catalyst is − 17.1 kcal/mol, which is similar to the value obtained for 1,2 coordination (− 17.7 kcal/mol). The corresponding complexation energy for the formation of the 2,1 styrene adduct with the Ti based species is − 6.6 kcal/mol, which is again very similar to the 1,2 styrene complexation (− 7.2 kcal/mol) and somewhat higher than the ethylene complexation energy (− 3.8 kcal/mol). The above results indicate that due to the higher steric hindrance in the titanocene catalyst respect to the zirconocene system, the 2,1 styrene complexation is less stable for the Ti than for the Zr based species.

Fig. 6 shows the principal structures found for the 2,1 styrene monomer insertion process into the $[Et_2(IndH_4)_2]ZrCH_3^+$ species along with their relative energies to the reactant. The geometrical parameters for these structures are presented in Table 5. The activation barrier calculated for the 2,1 styrene insertion is 11.0 kcal/mol, which is very similar to that found for the 1,2 process and very much

Table 5
Geometric parameters for 2,1styrene insertion into $[Et(IndH_4)]_2ZrCH_3^+$

	CpZrCp	Zr–Cp	Zr–Cp	Zr–C2est	$Zr–CH_3$	C1est–C2est	$C1est–CH_3$	Zr–Hγ	Zr–Hβ	Zr–Hα
π-Complex	125.9	2.252	2.240	3.227	2.261	1.375	3.305	–	–	–
Transition state	126.1	2.245	2.232	2.488	2.308	1.419	2.155	–	–	–
γ-Agostic product	125.9	2.245	2.220	2.283	2.615	1.569	1.575	2.255	–	–
β-Agostic product	127.9	2.232	2.185	2.322	3.820	1.525	1.539	–	2.140	–
α-Agostic product	126.5	2.219	2.214	2.297	4.714	1.543	1.544	–	–	2.283

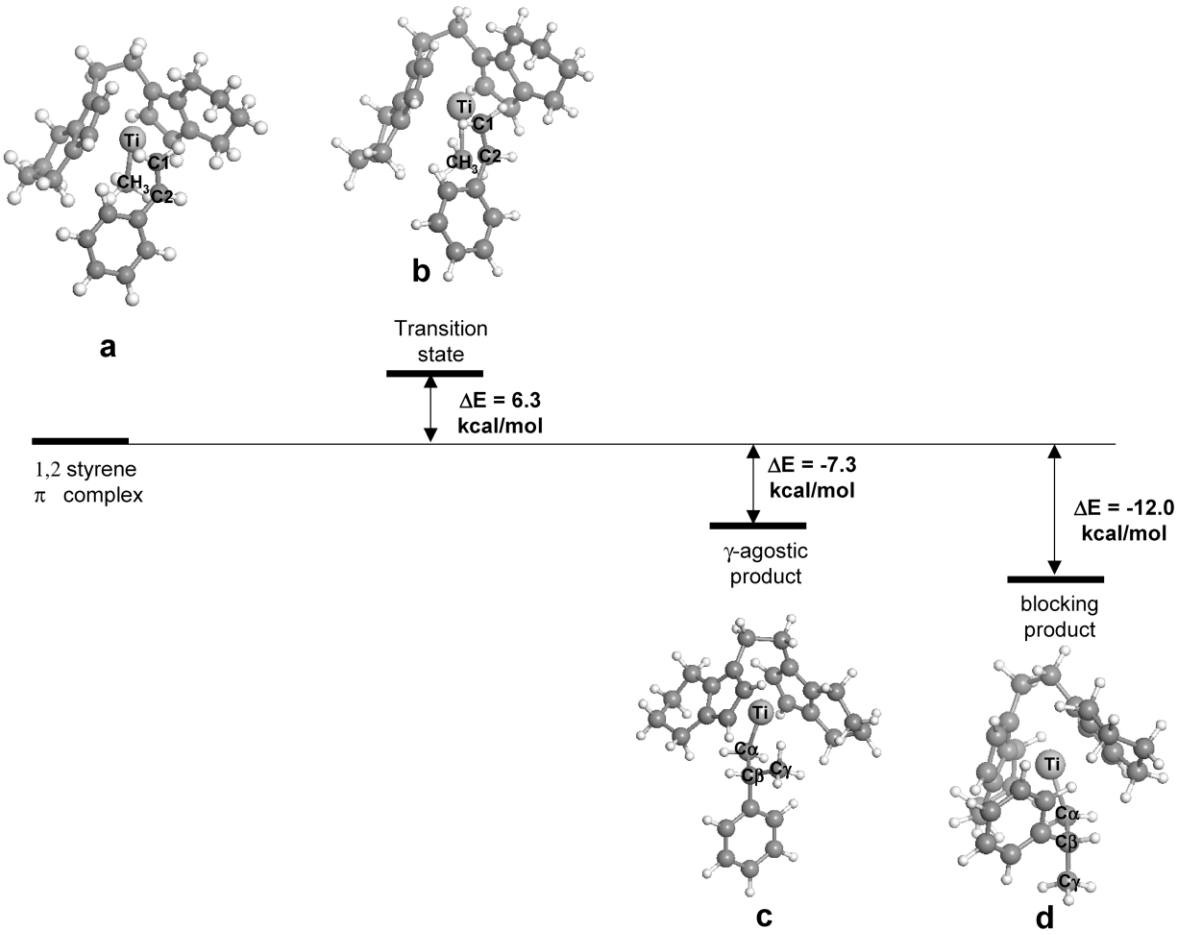

Fig. 5. Energy profile and structures for 1,2-styrene insertion into the *rac*-$Et_2(IndH_4)_2Ti(CH_3)^+$ catalyst.

larger than the activation barrier for ethylene insertion (2.1 kcal/mol). The kinetic product shows the characteristic γ-agostic interaction (Fig. 6c) and is only −1.8 kcal/mol more stable than the reactant adduct. Further rotation around the Cα–Cβ bond produces the β-agostic structure which is −5.3 kcal/mol lower in energy than the π-complex. This product is the known precursor of termination reactions such as β-elimination or β transfer to the monomer. On the other hand, the α-agostic conformer, obtained by rotation around the Zr–Cα bond, is the adequate precursor of the propagation step. In case of 2,1 styrene insertion the α-agostic product is 8.5 kcal/mol higher in energy than the β-agostic structure. Thus, the relative energy of the α-agostic product with respect to the reactant is 3.2 kcal/mol endothermic. The transition state for the rotation around the Zr–Cα bond presents the same problems as described for the same process in the ethylene insertion. The saddle point geometry is very close to the α-agostic product so that optimisation calculations tend to give a local minimum instead of a transition state. Therefore, it could be assumed that the rotation barrier from β to α-agostic product is in the order of 8.5 kcal/mol. Taking into account the whole process the limiting step in 2,1 styrene polymerization with the zirconocene catalyst is the monomer insertion with an energy barrier of 11.0 kcal/mol (see Fig. 6).

The relevant structures for 2,1 styrene insertion into the Ti based catalyst are presented in Fig. 7, and the geometrical parameters are given in Table 6. As it was described earlier the *si* coordination of the monomer to the metal centre is preferred over the *re* coordination. The transition state was

Table 6
Geometric parameters for 2,1 styrene insertion into $[Et(IndH_4)]_2TiCH_3^+$

	CpTiCp	Ti–Cp	Ti–Cp	Ti–C2est	Ti–CH_3	C1est–C2est	C1est–CH_3	Ti–Hγ	Ti–Hβ
π-Complex	130.5	2.098	2.083	3.251	2.150	1.370	3.047	–	–
Transition state	129.2	2.110	2.081	2.471	2.156	1.413	2.149	–	–
γ-Agostic product	129.7	2.100	2.059	2.176	2.677	1.558	1.557	2.140	–
β-Agostic product	129.7	2.101	2.059	2.176	3.894	1.558	1.557	–	2.224

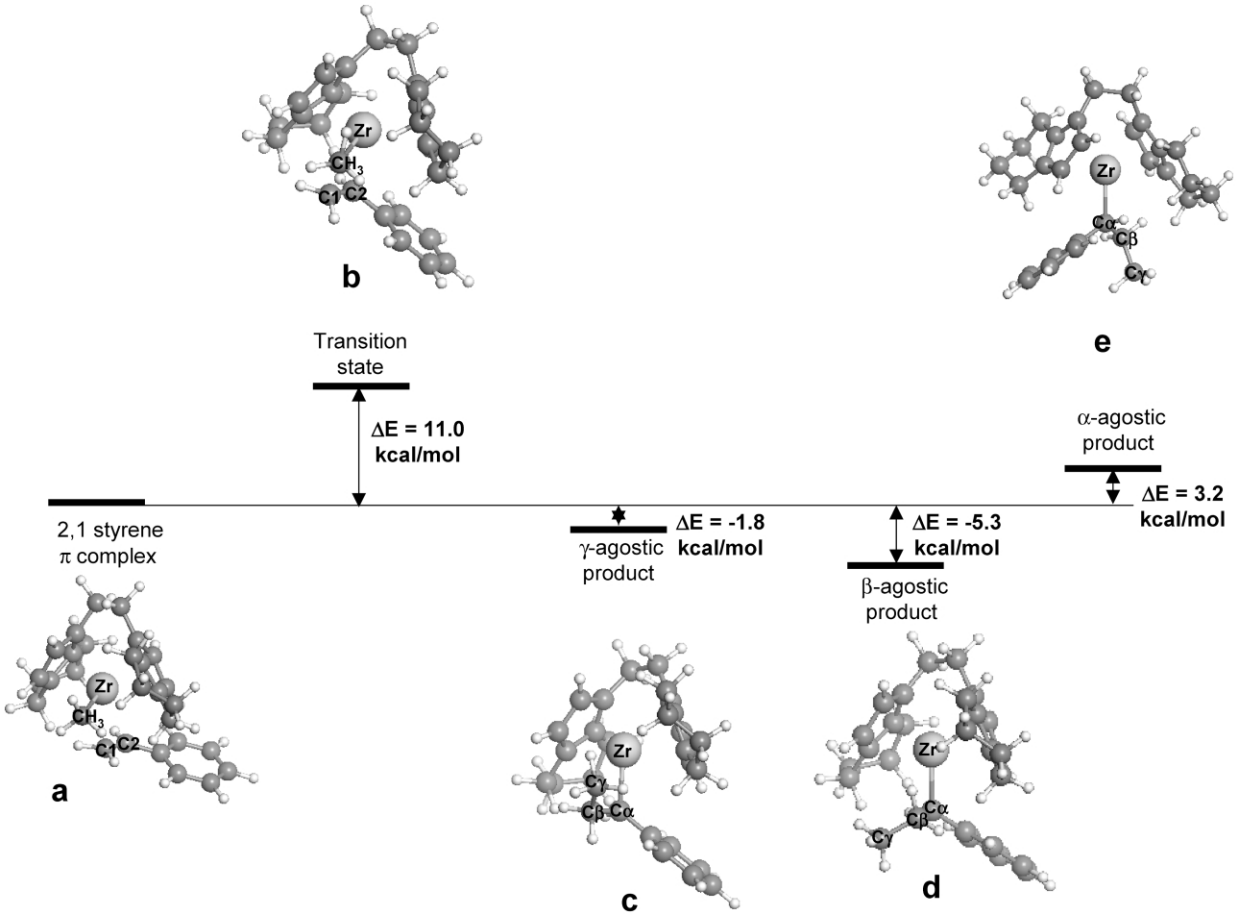

Fig. 6. Energy profile and structures for 2,1-styrene insertion into the *rac*-$Et_2(IndH_4)_2Zr(CH_3)^+$ catalyst.

located 7.4 kcal/mol above the reactant, so that the activation barrier is slightly higher than the corresponding to 1,2 styrene insertion (6.3 kcal/mol). The atom distances indicates that the saddle point is located earlier in the insertion path than the corresponding transition state for the 1,2 styrene insertion (see Tables 4 and 6). The γ-agostic product has an energy of −5.8 kcal/mol with respect to the π-complex. The relative exothermicity of the 2,1 styrene insertion reaction into the $[Et_2(IndH_4)_2]TiCH_3^+$ species is remarkably higher when it is compared to the same process but using the zirconocene catalyst (−5.8 vs. −1.8 kcal/mol). This product can rearrange to a more stable β-agostic conformation by rotation around the Cα–Cβ bond. The rotational barrier was estimated to be very small (1–2 kcal/mol) and the final β-agostic product is 9.1 kcal/mol lower in energy than the γ-agostic compound.

This very stable conformer is the precursor for the termination reactions, as it was commented above. A potential surface scan for the rotation around the Zr–Cα bond was performed to locate a structure presenting α-agostic interaction which is the species suitable for further monomer insertion. The large steric repulsion between the rotating growing polymer chain and the tetrahydroindenyl ligands prevent the formation of an α-agostic structure, so that further polymerization is not possible.

3.4. Ethylene–styrene copolymerization

Taking into account the results presented in the previous sections one can conclud that *rac*-$Et_2(IndH_4)_2Zr(CH_3)^+$ is the only species for the ethylene/styrene copolymerization. Furthermore, it has been assumed by different authors that the methyl group could be a valid model for a polyethylene growing chain. In this regard, the results presented in Part 2 are somehow describing the ethylene–styrene copolymerization step. The remaining styrene–ethylene copolymerization reaction will be presented here.

Fig. 8 shows the energy profile for the insertion of an ethylene monomer into the α-agostic conformer produced after 2,1 styrene insertion. The complexation energy is −12.6 kcal/mol, which is slightly below the value obtained for the initial ethylene insertion (−14.3 kcal/mol, see Part 1). The transition state corresponding to the ethylene insertion reaction is 1.9 kcal/mol above the reactant, being 0.4 kcal/mol lower than the energy barrier for the initial ethylene insertion. The geometries of both transition states are very similar as shown in Tables 1 and 7. The γ-agostic product is 13.1 kcal/mol lower in energy than the reactant, which is similar to the value obtained for the first ethylene insertion (−12.9 kcal/mol, see Fig. 2c). The β-agostic conformer is again the most stable product with 6.5 kcal/mol

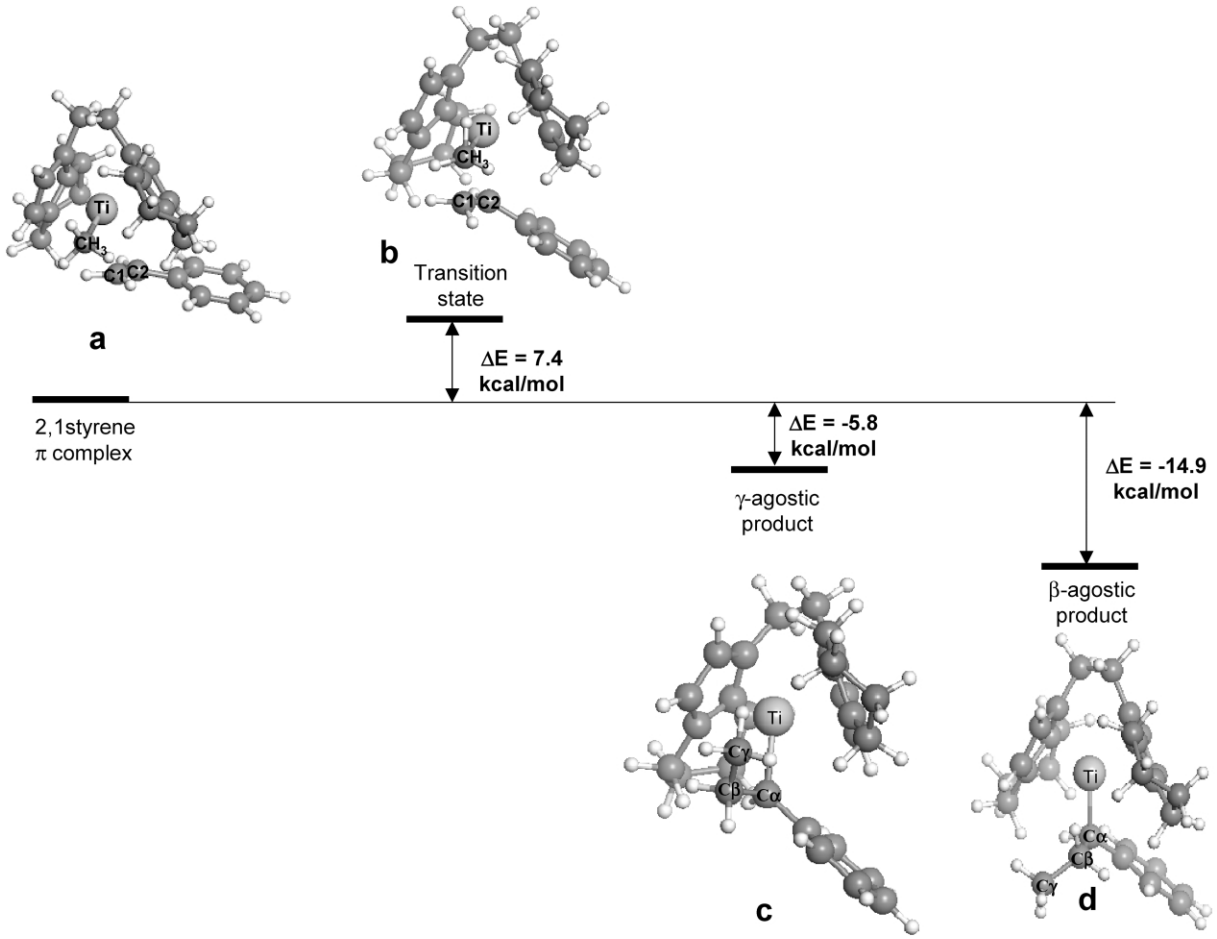

Fig. 7. Energy profile and structures for 2,1-styrene insertion into the *rac*-$Et_2(IndH_4)_2Ti(CH_3)^+$ catalyst.

lower in energy than the γ-agostic structure. The β-agostic conformer obtained here is more stable than the equivalent conformer in the initial ethylene insertion as the difference in energy relative to the γ-agostic structure is higher than the one found for ethylene polymerization (3.1 kcal/mol, see Fig. 2). The α-agostic structure produced by rotation of the alkyl chain around the Zr–Cα bond is 9.0 kcal/mol above the β-agostic energy, which is higher than the same process in the ethylene homopolymerization case (7.8 kcal/mol, see Fig. 2). Based on these results and assuming that the limiting step in olefin propagation is the rotation of the growing polymer chain around the metal–Cα bond, the styrene monomer incorporation into the forming copolymer will reduce the activity of the catalyst.

4. Conclusions

The copolymerization of ethylene and styrene is a competitive process between the two monomers. The complexation energies calculated in this work for both monomers reveal that styrene coordination to the metal atom is preferred over the ethylene complexation, being about 3 kcal/mol for both Ti and Zr metallocene systems. The π-complexes formed by either ethylene or styrene and the *rac*-$Et_2(IndH_4)_2Zr(CH_3)^+$ catalyst are much more stable than those produced with the *rac*-$Et_2(IndH_4)_2Ti(CH_3)^+$ system. This can be explained by the higher steric congestion around the Ti compared to the Zr atom.

Looking at the complete paths for the insertion reactions,

Table 7
Geometric parameters for ethylene insertion into $[Et_2(IndH_4)]_2Zr(CH(Phe)CH_2CH_3)^+$

	CpZrCp	Zr–Cp	Zr–Cp	Zr–C1et	Zr–Cest	C1et–C2et	C2et–Cest	Zr–Hγ	Zr–Hβ	Zr–Hα
π-Complex	125.3	2.259	2.262	2.826	2.333	1.367	2.942	–	–	–
Transition state	124.8	2.248	2.260	2.421	2.452	1.411	2.325	–	–	–
γ-Agostic product	126.0	2.218	2.227	2.259	2.983	1.553	1.562	2.249	–	–
β-Agostic product	127.6	2.203	2.215	2.270	3.911	1.521	1.556	–	2.183	–
α-Agostic product	128.5	2.196	2.204	2.217	4.760	1.527	1.565	–	–	2.269

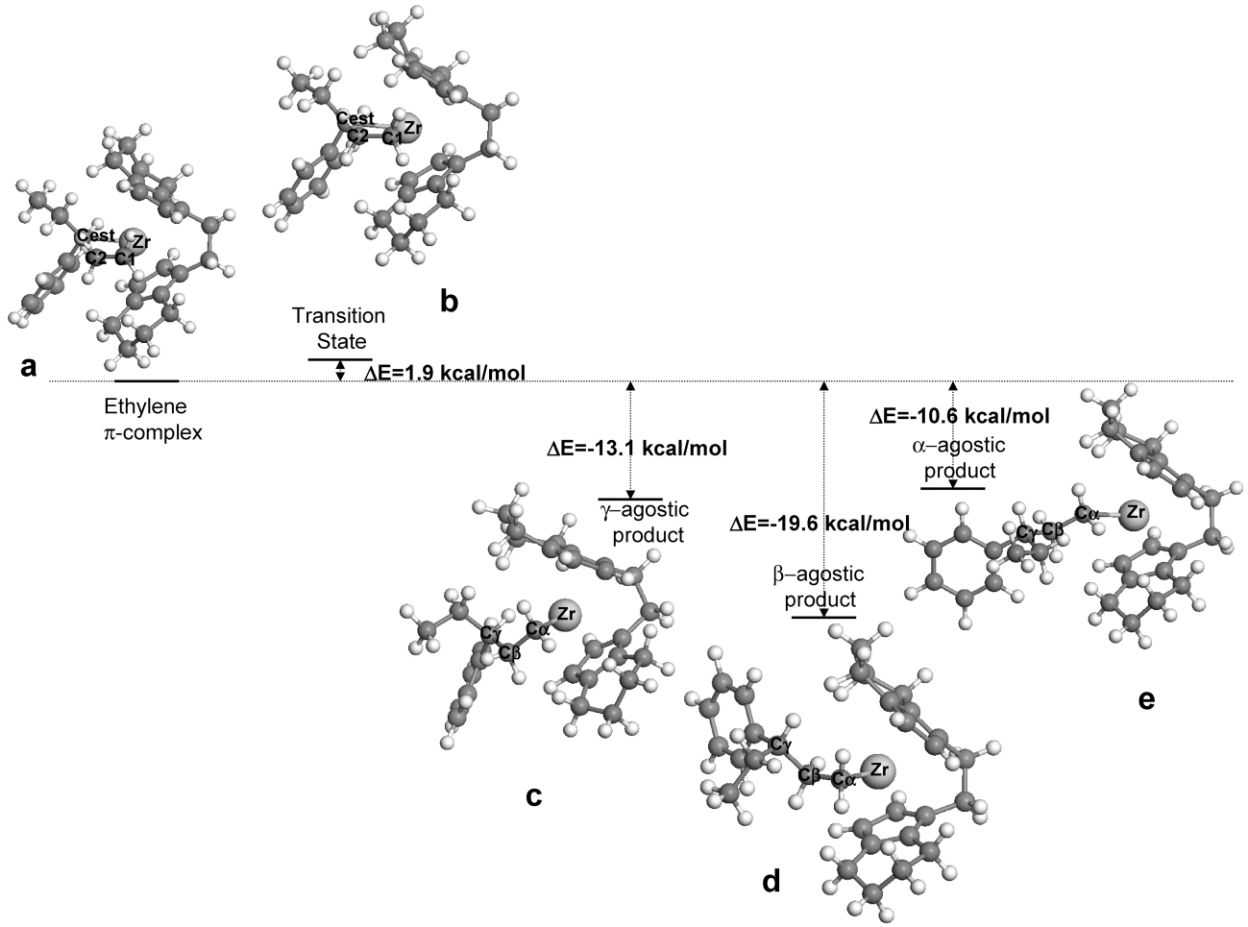

Fig. 8. Energy profile and structures for ethylene insertion into the *rac*-$Et_2(IndH_4)_2Zr(CH(Phe)CH_2CH_3)^+$ species produced after 2,1-styrene insertion.

it could be settled than in ethylene polymerization the controlling step must be the alkyl chain rotation around the metal–Cα bond. In this sense ethylene polymerization is much easier with the zirconocene than with the titanocene system, in agreement with the experimental findings [16].

There is no appreciable difference between primary and secondary styrene complexation and insertion. However, the most stable product formed after primary insertion gives rise to a compound in which the active site is blocked by the phenyl ring of the growing polymer chain, avoiding further polymerization. This blocking conformer is formed by rotation of the alkyl chain around the Cα–Cβ bond. This result gives an explanation to the experimental fact that primary styrene insertion is very unlikely to occur [4,5].

It was also found that the secondary insertion is more difficult than ethylene polymerization using the *rac*-$Et_2(IndH_4)_2Zr(CH_3)^+$ catalyst due to the large activation barrier and to the small relative stability of the products with respect to the reactants. In fact the α-agostic conformer is higher in energy than the π-complex. Therefore the incorporation of styrene in the copolymer will be very low as compared to ethylene polymerization, as it has been experimentally found with for other ansa-metallocene catalysts [4,5]. The insertion of styrene into the growing chain gives rise to a decrease in the catalytic activity according also with the experimental results [4,5]. The energy barrier for the controlling step in the ethylene insertion process, i.e. the alkyl chain rotation, is higher after 2,1 styrene monomer has been inserted in comparison to the ethylene polymerization step.

In the titanocene system the secondary styrene insertion process gives rise to structures which are more suitable for termination than for polymerization reactions. Furthermore, styrene complexation and insertion in the Ti based system are more likely to occur than with the ethylene monomer so that the active centres are easily blocked.

Acknowledgements

Thanks are due to the CICYT (Grant MAT2002-01242) for financial support. The authors also acknowledge Repsol-YPF, Spain for their permission to publish these data.

References

[1] Natta G, Pino P, Mantica E, Danusso F, Mazzanti G, Peraldo M. Chim Ind 1956;38:124.

[2] Natta G, Danusso F, Sianesi D. Makromol Chem 1958;28:253.
[3] Soga K, Lee D-H, Yenihara H. Polym Bull Berlin 1988;20:237.
[4] Pellecchia C, Oliva L. Rubber Chem Technol 1999;72:553.
[5] Oliva L, Caporaso L, Pellechia C, Zambelli A. Macromolecules 1995; 28:4665.
[6] Thomann Yi, Sernetz FG, Thomann R, Kressler, Mühlhaupt R. Macromol Chem Phys 1997;198:739.
[7] Sernetz FG, Mühlhaupt R, Amor F, Eberle T, Okuda J. J Polym Sci, Part A: Polym Chem Ed 1997;35:1571.
[8] Lee D-G, Yoon K-B, Kim H-J, Woo S-S, Noh SK. J. Appl Polym Sci 1998;67:2187.
[9] Sernetz FG, Mühlhaupt R, Fokken S, Okuda J. Macromolecules 1997; 30:1562.
[10] Inoue N, Shimura T. Polym Prepr Jpn 1993;42:2292.
[11] Arai T, Ohsu T. Suzuki Polym Prepr 1997;38:349.
[12] Oliva L, Izzo L, Longo P. Macromol Rapid Commun 1996;17:745.
[13] Oliva L, Longo P, Izzo L, Di Serio M. Macromolecules 1997;30: 5616.
[14] Arai T, Ohsut T, Suzuki S. Macromol Rapid Commun 1998;19:327.
[15] Muñoz-Escalona A, Cruz V, Mena N, Martínez S, Martínez-Salazar J. Polymer 2002;43:7017.
[16] Expósito T, Muñoz-Escalona A, Cruz V, Martínez-Salazar J. To be published.
[17] Vosko H, Wil L, Nusair M. Can J Phys 1980;58:1200.
[18] Becke AD. Phys Rev A 1988;38:3098.
[19] Perdew JP. Phys Rev B 1986;34:7406.
[20] Hay PJ, Wadt WR. J Chem Phys 1985;82:299.
[21] Ramos J, Cruz V, Muñoz-Escalona A, Martínez-Salazar J. Polymer 2000;41:6161.
[22] Lohrenz JCW, Woo TK, Ziegler T. J Am Chem Soc 1995;117:12793.
[23] Lohrenz JCW, Woo TK, Fan L, Ziegler T. J Organomet Chem 1995; 497:91.
[24] Margl P, Deng L, Ziegler T. J Am Chem Soc 1998;120:5517.
[25] Froese RDJ, Musaev DG, Morokuma K. J Am Chem Soc 1998;120: 1581.
[26] Reddy SS, Sivaram S. Prog Polym Sci 1995;20:309.
[27] Kaminsky W. In: Kricheldorf HR, editor. Handbook of polymer synthesis. Part A. Marcel Dekker, Inc., New York; 1992.